(Received 5 November 2025, Accepted 9 December 2025, Scheduled 29 December 2025)

A Model-Free Adaptive Control for PMSM Using Multi-Innovation Improved EKF

Kaihui Zhao[1], Youzhuo Duan[1], Jie Xiong[1,*], Lingxuan Tu[1], and Yishan Huang[2]

[1]*School of Transportation and Electrical Engineering, Hunan University of Technology, China*
[2]*CRRC Electric Vehicle Co., Ltd., China*

ABSTRACT: Permanent magnet synchronous motor (PMSM) used in high-end applications has stringent control performance requirements. However, harsh environments, complex operating conditions, and nonlinear parameter variations can compromise model adaptability, which undermines system reliability and precision. This paper proposes a model-free adaptive control (MFAC) method that utilizes a Multi-Innovation Improved Extended Kalman Filter (MIIEKF) algorithm for prediction and update to enhance system reliability and accuracy. First, the proposed method transforms the PMSM model into a compact-form dynamic linearization (CFDL) data model, which mitigates the need for precise mathematical modeling. Next, an improved Extended Kalman Filter (IEKF) algorithm is used to predict and update the pseudo partial derivative (PPD) in real-time. This resolves its estimation dependency and compensates for data model inaccuracies. Then, the IEKF algorithm is optimized by using Multi-Innovation identification theory to ensure rapid state convergence. Finally, experimental validation confirms that the proposed method significantly improves the convergence rate, reduces chattering, and achieves efficient data-driven control compared to PI control and conventional model-free adaptive control.

1. INTRODUCTION

PMSMs are predominantly adopted for high-performance applications in industrial contexts [1], benefiting from their superior efficiency and compact design [2]. Although conventional proportional-integral (PI) control remains popular for its simplicity, it often falls short in meeting high-precision demands [3]. While model-based robust control methods have been developed to address these limitations [4], their performance tends to degrade under system uncertainties and modeling complexity. This has spurred growing interest in model-free solutions.

Existing model-free control methods based on an ultra-local model can capture system behavior locally but lack a comprehensive representation of global dynamics [5]. A model-free predictive control method was designed based on an ultra-local model, significantly reducing speed overshoot and oscillation amplitude, but still failed to fully characterize the system state [6].

A data-driven model-free adaptive control (MFAC) utilizes real-time input-output data to construct dynamic linearizations such as the compact-form dynamic linearization (CFDL) [7]. A CFDL-based MFAC integrated with multi-vector predictive current control is proposed to enable adaptive speed regulation [8]. However, the CFDL has exhibited limited adaptability and weak disturbance rejection capabilities due to its reliance on real-time pseudo-partial derivative (PPD) estimation [9].

The employment of an extended Kalman filter (EKF) has been shown to enhance the accuracy of state estimation and the robustness of the system. A method integrating the model reference adaptive approach with EKF-based current noise compensation has been demonstrated to achieve precise motor speed estimation while suppressing noise [10]. Nevertheless, EKF is constrained by high computational cost and linearization errors [11]. Meanwhile, the multi-innovation identification theory (MIIT) overcomes the limitations of single-innovation recursion by incorporating historical data vectors, thereby improving convergence speed and estimation accuracy [12].

This paper proposes a multi-innovation improved EKF-based MFAC (MIIEKF-MFAC) method to enhance the robustness and stability of PMSM drives under varying operating conditions.

The primary contributions of this research are outlined below:

(i) The integration of MFAC and MIIEKF achieves model-free control with high-precision state prediction. This synergy enables real-time estimation and updates while substantially reducing reliance on PPD estimation, thereby considerably enhancing dynamic robustness.

(ii) The method reduces computational complexity and resource consumption significantly by replacing the covariance matrix in the conventional EKF with a single tuning parameter.

(iii) The method incorporates the merits of the MIIT, such as elevated adjustment flexibility and superior tracking of time-varying parameters.

The structure of this paper is outlined below. Section 2 details the CFDL model-free adaptive control (CFDL-MFAC)

* Corresponding author: Jie Xiong (2136329325@qq.com).

framework for PMSM. Section 3 first elaborates on the IEKF-Based PPD prediction-update (IEKF-PPD) Algorithm, then introduces the multi-innovation optimized scheme (MIIEKF-PPD) and presents its comprehensive architecture. Section 4 provides a stability analysis of the proposed algorithm. Section 5 presents the experimental verification of the proposed strategy's effectiveness. Section 6 concludes with a summary of key findings.

2. CFDL-MFAC FOR PMSM

According to the MFAC theory, the PMSM system can be modeled as:

$$n(k+1) = f\left(n(k),\ldots,n(k-b_y),i_q(k),\ldots,i_q(k-b_u)\right), \tag{1}$$

where $n(k)$ and $i_q(k)$ represent the output speed and input current of the PMSM system at time k, respectively; b_y and b_u are two unknown positive integers.

Assumption 1 *The system (1) is both observable and controllable. That is, when the desired output signal $n^*(k+1)$ is bounded, it is always possible to construct a finite control input that ensures the system output asymptotically tracks the desired signal.*

Assumption 2 *The system (1) satisfies a generalized Lipschitz condition, meaning that for any time instant k and $\Delta i_q(k) \neq 0$, the following holds:*

$$|\Delta n(k+1)| \leq b\,|\Delta i_q(k)|, \tag{2}$$

where $\Delta n(k+1) = n(k+1)-n(k)$; $\Delta i_q(k) = i_q(k)-i_q(k-1)$; and b is a positive constant.

Assumption 3 *At any time instant k, where $\Delta i_q(k) \neq 0$, restricted adjustments to the input of the PMSM system will not cause its output to grow or decay unbounded; that is, $|\phi(k)| \leq b$, where $\phi(k)$ denotes the pseudo partial derivative.*

Under Assumptions 1–3, with the PMSM operating under the $i_d = 0$ control strategy, whenever $\Delta i_q(k) \neq 0$, there must exist a $\phi(k)$ such that the PMSM system can be represented by the following dynamically linearized data model:

$$\Delta n(k+1) = \phi(k)\Delta i_q(k). \tag{3}$$

The CFDL-based MFAC (CFDL-MFAC) relies solely on the input of the current time step. The control procedure of the CFDL-MFAC is outlined below:

i) Estimate the PPD using the I/O data of system (3):

$$\begin{aligned}\phi(k) &= \phi(k-1) + \frac{\eta\Delta i_q(k-1)\Delta n(k)}{\mu+\Delta i_q(k-1)^2} \\ &\quad - \frac{\eta\Delta i_q(k-1)\phi(k-1)\Delta i_q(k-1)}{\mu+\Delta i_q(k-1)^2},\end{aligned} \tag{4}$$

where $\mu > 0$ is a weighting factor, and $\eta \in (0\ ,\ 1]$ represents the step-size factor.

ii) Introduce a reset mechanism into the PPD estimation algorithm:

$$\phi(k) = \phi(1), \begin{cases} |\phi(k)| \leq \varepsilon \\ |\Delta i_q(k-1)| \leq \varepsilon \\ \text{sign}((\phi(k) \neq \text{sign}(\phi(1)) \end{cases}, \tag{5}$$

where ε is a sufficiently small positive constant.

iii) Derive the control law based on the control input criterion function:

$$i_q^*(k) = i_q(k-1) + \frac{\rho\phi(k)}{\lambda+|\phi(k)|^2}\left(n^*(k+1)-n(k)\right), \tag{6}$$

where $\lambda > 0$ and $\rho \in (0,1]$ are control parameters. i_q^* denotes the reference output current.

Remark 1 *The dynamically linearized data model (3) relies solely on the system I/O data and contains no explicit or implicit model information of the controlled plant. Thus, the CFDL-MFAC constitutes a data-driven approach. Consequently, the aforementioned assumptions are easily satisfied in practical PMSM systems. However, errors in the data model may still arise due to dynamic linearization approximations, noise disturbances, and PPD estimation deviations.*

Assumption 4 *The data model error, $d(k)$ is bounded; that is, there exists a constant $b_d > 0$ such that $|d(k)| < b_d$.*

3. DESIGN OF MFAC FOR PMSM BASED ON MIIEKF

To counteract the limitations of CFDL-MFAC, such as residual model errors and accumulating PPD deviations, this paper proposes an IEKF-based prediction-update mechanism integrated with a multi-innovation algorithm. This significantly boosts the system's response speed.

3.1. IEKF-PPD

Considering both data model errors and estimation inaccuracies, the one-step-ahead prediction of the PPD using the modified projection estimation algorithm is described as

$$\begin{cases} \phi_m(k) = \phi_m(k-1) + \dfrac{\eta\Delta i_q(k-1)\Delta n(k)}{\mu+\Delta i_q(k-1)^2} \\ \qquad\qquad - \dfrac{\eta\phi_m(k-1)\Delta i_q(k-1)^2}{\mu+\Delta i_q(k-1)^2} + w(k-1) \\ \phi(k) = \phi_m(k) + v(k), \end{cases} \tag{7}$$

where $\phi_m(k) \in \mathrm{R}$ represents the actual PPD under the CFDL; $\phi(k) \in \mathrm{R}$ denotes the estimated PPD obtained via the modified projection algorithm; $w(k) \in \mathrm{R}$ is the process noise arising from data model errors in the dynamically linearized system; $v(k) \in \mathrm{R}$ refers to the estimation error introduced by the modified projection algorithm together with external disturbances; $\mu > 0$ is a weighting factor and $\eta \in (0,1]$ represents the step-size factor.

The following assumptions are made for system (7):

Assumption 5 *The noise terms $w(k)$ and $v(k)$ are defined as mutually uncorrelated white noise sequences of zero mean, possessing variances Q and R, respectively.*

$$\mathrm{E}[w(k)] = 0, \quad \mathrm{E}[w(k)^2] = Q,$$

$$\mathrm{E}[v(k)] = 0, \quad \mathrm{E}[v(k)^2] = R, \quad \mathrm{E}[w(k)v(k)] = 0.$$

Remark 2 *In practical applications involving complex error noises arising from diverse sources with unknown probability distributions, Gaussian white noise can serve as an effective approximation. This approach aligns with the fundamental noise characteristics of the classical Kalman filter, thereby establishing the practical feasibility of Assumption 5.*

Within the framework of the dynamically linearized model, let $\hat{\phi}(k|k) = \mathrm{E}^*[\phi_m(k)/\phi(k)]$ denote the linear minimum variance estimate of the actual PPD value $\phi_m(k)$ based on the estimated PPD value $\phi(k)$.

Lemma 1 *The minimum variance estimate has the property of linearity. Specifically, if the linear minimum variance estimate of the actual data φ given the quantity ζ is $\mathrm{E}^*[\varphi/\zeta]$, then for any deterministic matrix $\mathbf{F}$ and deterministic vector $\boldsymbol{\omega}$, the linear minimum variance estimate of $\mathbf{F}\varphi+\omega$ given the same quantity ζ is given by*

$$\mathrm{E}^*\left[\frac{\mathbf{F}\varphi+\boldsymbol{\omega}}{\zeta}\right] = \mathbf{F}\mathrm{E}^*\left[\frac{\varphi}{\zeta}\right] + \boldsymbol{\omega}. \tag{8}$$

Theorem 1 *Under the condition that system (7) satisfies Assumption 5, the IEKF algorithm performs real-time prediction and update utilizing the initial pseudo partial derivative value with an initial error covariance $P(0|0) = P(0)$.*

The detailed procedure for PPD prediction and updating via the IEKF is as follows:

1) One-step-ahead PPD prediction:

$$\hat{\phi}(k|k-1) = \hat{\phi}(k-1|k-1) + \frac{\eta\Delta i_q(k-1)\Delta n(k)}{\mu+\Delta i_q(k-1)^2} - \frac{\eta\hat{\phi}(k-1|k-1)\Delta i_q(k-1)^2}{\mu+\Delta i_q(k-1)^2}. \tag{9}$$

2) One-step prediction error covariance:

$$P(k|k-1) = \left(1 - \frac{\eta\Delta i_q(k-1)^2}{\mu+\Delta i_q(k-1)^2}\right)^2 P(k-1|k-1) + Q. \tag{10}$$

3) Compute the IEKF gain:

$$K(k) = \frac{P(k|k-1)}{P(k|k-1)+R}. \tag{11}$$

4) Optimal estimate of the PPD Value:

$$\hat{\phi}(k|k) = \hat{\phi}(k|k-1) + K(k)[\phi(k) - \hat{\phi}(k|k-1)]. \tag{12}$$

5) Update the estimation error covariance:

$$P(k|k) = [1-K(k)]\,P(k|k-1). \tag{13}$$

Proof 1 *The one-step-ahead prediction involves estimating the output value at time k based on the estimated value at time $k-1$. That is, it constructs the linear minimum variance estimate of $\phi_m(k-1)$ using the actual PPD data $\{\phi(1),\phi(2),\ldots,\phi(k-1)\}$ from the first $k-1$ time instants of the system.*

$$\begin{aligned}\hat{\phi}(k|k-1) &= \mathrm{E}^*\left[\frac{\phi_m(k)}{\phi(1),\phi(2),\ldots,\phi(k-1)}\right] \\ &= \mathrm{E}^*\left[\frac{\phi_m(k-1)}{\phi(1),\phi(2),\ldots,\phi(k-1)}\right] \\ &\quad + \mathrm{E}^*\left[\frac{\frac{\eta\Delta i_q(k-1)\Delta n(k)}{\mu+\Delta i_q(k-1)^2}}{\phi(1),\phi(2),\ldots,\phi(k-1)}\right] \\ &\quad - \mathrm{E}^*\left[\frac{\frac{\eta\Delta i_q(k-1)^2\phi_m(k-1)}{\mu+\Delta i_q(k-1)^2} + w(k-1)}{\phi(1),\phi(2),\ldots,\phi(k-1)}\right].\end{aligned} \tag{14}$$

It follows from Lemma 1 that

$$\begin{aligned}\hat{\phi}(k|k-1) &= \mathrm{E}^*\left[\frac{\phi_m(k-1)}{\phi(1),\phi(2),\ldots,\phi(k-1)}\right] \\ &\quad - \mathrm{E}^*\left[\frac{\phi_m(k-1)}{\phi(1),\phi(2),\ldots,\phi(k-1)}\right] \\ &\quad \frac{\eta\Delta i_q(k-1)^2}{\mu+\Delta i_q(k-1)^2} \\ &\quad + \mathrm{E}^*\left[\frac{w(k-1)}{\phi(1),\phi(2),\ldots,\phi(k-1)}\right] \\ &\quad + \frac{\eta\Delta i_q(k-1)\Delta n(k)}{\mu+\Delta i_q(k-1)^2}\end{aligned} \tag{15}$$

Within the framework of the modified projection algorithm, (7) indicates that the PPD value $\phi(k)$ is mutually independent of the process noise $w(k-1)$. Due to the zero mean property $E[w(k)] = 0$ stated in Assumption 5, the one-step-ahead prediction of the PPD value is derived as follows:

$$\hat{\phi}(k|k-1) = \hat{\phi}(k-1|k-1) + \frac{\eta\Delta i_q(k-1)\Delta n(k)}{\mu+\Delta i_q(k-1)^2} - \frac{\eta\hat{\phi}(k-1|k-1)\Delta i_q(k-1)^2}{\mu+\Delta i_q(k-1)^2}. \tag{16}$$

To ensure that parameter estimation converges and to prevent parameter perturbation, a reset mechanism similar to that used in CFDL-MFAC is introduced into the one-step-ahead PPD prediction:

$$\hat{\phi}(k|k-1) = \hat{\phi}(1|0), \begin{cases} |\hat{\phi}(k|k-1)| \le \varepsilon \\ |\Delta i_q(k-1)| \le \varepsilon \\ \mathrm{sign}(\hat{\phi}(k|k-1)) \ne \mathrm{sign}(\hat{\phi}(1|0)). \end{cases} \tag{17}$$

The error introduced by substituting the one-step-ahead predicted value $\hat{\phi}(k|k-1)$ for the actual system PPD value $\phi_m(k)$ is given by

$$e_m(k|k-1) = \phi_m(k) - \hat{\phi}(k|k-1). \tag{18}$$

The estimation residual resulting from substituting the one-step-ahead predicted value $\hat{\phi}(k|k-1)$ for the PPD estimate $\phi(k)$ of the modified projection algorithm is defined as follows:

$$\begin{aligned} e_c(k|k-1) &= \phi(k) - \hat{\phi}(k|k-1) \\ &= \phi_m(k) - \hat{\phi}(k|k-1) + v(k) \\ &= e_m(k|k-1) + v(k). \end{aligned} \tag{19}$$

A weighted adjustment is applied to the residual $e_c(k|k-1)$ to correct the one-step-ahead prediction $\hat{\phi}(k|k-1)$, producing the final updated PPD value $\hat{\phi}(k|k)$.

$$\begin{aligned} \hat{\phi}(k|k) &= \hat{\phi}(k|k-1) + K(k)e_c(k|k-1) \\ &= \hat{\phi}(k|k-1) + K(k)[\phi(k) - \hat{\phi}(k|k-1)], \end{aligned} \tag{20}$$

where $K(k) \in [0,1]$ is the gain coefficient for $e_c(k|k-1)$, denoting the filter gain.

Define the predicted-updated error as $e_m(k|k) = \phi_m(k) - \hat{\phi}(k|k)$. The gain coefficient $K(k)$ is selected to minimize the mean square error $P(k|k) = \mathrm{E}[e_m(k|k)^2]$. From Equations (7) and (20), we obtain

$$\begin{aligned} e_m(k|k) &= \phi_m(k) - \hat{\phi}(k|k) \\ &= [1 - K(k)]\, e_m(k|k-1) - K(k)v(k). \end{aligned} \tag{21}$$

From Assumption 5, it follows that

$$\begin{aligned} P(k|k) &= \mathrm{E}[e_m(k|k-1)^2 - 2K(k)e_m(k|k-1)^2 \\ &\quad + K(k)^2 v(k)^2 + K(k)^2 e_m(k|k-1)^2 \\ &\quad + 2(1-K(k))e_m(k|k-1)K(k)v(k)] \\ &= P(k|k-1) - 2K(k)P(k|k-1) \\ &\quad + K(k)^2 R + K(k)^2 P(k|k-1), \end{aligned} \tag{22}$$

where

$$\begin{aligned} e_m(k|k-1) &= \phi_m(k) - \hat{\phi}(k|k-1) \\ &= \left(1 - \frac{\eta \Delta i_q(k-1)^2}{\mu + \Delta i_q(k-1)^2}\right) e_m(k-1|k-1) \\ &\quad + w(k-1). \end{aligned} \tag{23}$$

Given the mean square error and Assumption 5, it can be derived that

$$\begin{aligned} & P(k|k-1) \\ &= \mathrm{E}\left[\left(\left(1 - \frac{\eta \Delta i_q(k-1)^2}{\mu + \Delta i_q(k-1)^2}\right) e_m(k-1|k-1) + w(k-1)\right)^2\right] \\ &= \left(1 - \frac{\eta \Delta i_q(k-1)^2}{\mu + \Delta i_q(k-1)^2}\right)^2 P(k-1|k-1) + Q. \end{aligned} \tag{24}$$

Differentiating (22) with respect to $K(k)$ and setting the derivative to zero yields the filter gain:

$$K(k) = \frac{P(k|k-1)}{P(k|k-1) + R}. \tag{25}$$

Furthermore, substituting (25) into (22) yields

$$\begin{aligned} P(k|k) &= P(k|k-1) - 2P(k|k-1)\frac{P(k|k-1)}{P(k|k-1)+R} \\ &\quad + (P(k|k-1) + R)\left(\frac{P(k|k-1)}{P(k|k-1)+R}\right)^2 \\ &= [1 - K(k)]P(k|k-1). \end{aligned} \tag{26}$$

By integrating Equations (16), (20), (24), (25), and (26), the IEKF prediction-update equation set is thus proven.

3.2. MIIEKF-PPD

Although the single-innovation method in (12) updates the model using only the current innovation, which aligns with the CFDL conceptually, it underutilizes available data. MIIT addresses this issue by integrating a series of past innovations within a sliding window. This strategy is analogous to PFDL and enables a more thorough and precise system identification.

$$\theta(t) = \theta(t-1) + \mathbf{T}_p(t)\mathbf{E_p}(t), \tag{27}$$

$$\mathbf{E_p^T}(t) = [e(t), e(t-1), \ldots, e(t-p+1)], \tag{28}$$

where θ is the parameter estimation vector; $\mathbf{T_p}(t) \in \mathrm{R}^{1\times p}$ denotes the gain matrix; $\mathbf{E_p}(t) \in \mathrm{R}^{p\times 1}$ represents the Multi-Innovation vector; and $p \geq 1$ indicates the length of the Multi-Innovation vector.

The Multi-Innovation vector $\mathbf{E_p}(k)$ is defined as:

$$\begin{aligned} \mathbf{E_p}(k) &= \begin{bmatrix} e_c(k|k-1) \\ e_c(k-1|k-2) \\ \vdots \\ e_c(k-p+1|k-p) \end{bmatrix} \\ &= \begin{bmatrix} \phi(k) - \hat{\phi}(k|k-1) \\ \phi(k-1) - \hat{\phi}(k-1|k-2) \\ \vdots \\ \phi(k-p+1) - \hat{\phi}(k-p+1|k-p) \end{bmatrix}. \end{aligned} \tag{29}$$

Extend the gain coefficient $\mathbf{K_p}(k)$ into a Multi-Innovation gain matrix

$$\mathbf{K_p}(k) = \begin{bmatrix} K(k) \\ K(k-1) \\ \vdots \\ K(k-p+1) \end{bmatrix}. \tag{30}$$

To mitigate the cumulative disturbance caused by outdated data in the Kalman prediction, a forgetting factor is introduced. This balances the influence of historical and recent data, thus improving the update accuracy.

The forgetting factor matrix is defined as:

$$\alpha = \text{diag}\left(\lambda_1, \lambda_2, \ldots, \lambda_p\right), \tag{31}$$

where the weighting matrix for the forgetting factors can be selected as

$$\begin{cases} \lambda_1 = 1 \\ \lambda_2 = \lambda_3 = \ldots = \lambda_p = \frac{\beta}{p-1} \end{cases}, \tag{32}$$

where β denotes the historical forgetting rate, which is bounded by $0 \leq \beta \leq 1$.

Substituting (31), (30), and (29) into (12) yields:

$$\hat{\phi}_{MI}(k|k) = \hat{\phi}(k|k-1) + \alpha \sum_{i=1}^{p} E_p(k) K_p(k). \tag{33}$$

Thus, synthesizing (16), (24), (25), (26), and (33) establishes the PPD equations based on the multi-innovation improved extended Kalman filter prediction-update. Substituting $\hat{\phi}_{MI}(k|k)$ for $\phi(k)$ in CFDL-MFAC yields the proposed MIIEKF-MFAC algorithm.

Figure 1 illustrates the MIIEKF-based MFAC system. Figure 2 shows the overall algorithm structure.

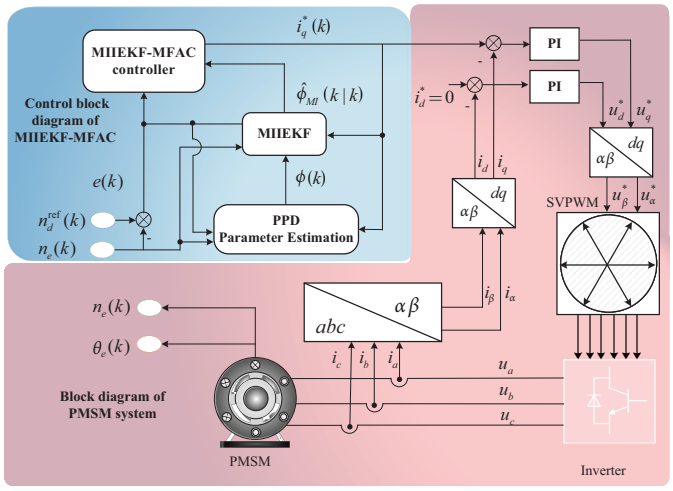

FIGURE 1. Block diagram of the MFAC system based on MIIEKF.

The steps of the MIIEKF-PPD algorithm are described below, using the prediction of the PPD value at time k as an example.

Step 1: Based on the dynamic linearization model of MFAC, the time-varying parameter PPD is calculated.

Step 2: Prediction and Update based on MIIEKF information: Taking the PPD data $\phi(k-1)$ output by the projection algorithm at time $k-1$ and the corresponding optimal PPD estimate $\hat{\phi}_{MI}(k-1|k-1)$ as the baseline inputs, the predicted value $\hat{\phi}(k|k-1)$ of the PPD at the current moment is obtained through the prediction mechanism of MIIEKF. This is then used to calculate the MIIEKF gain and, combined with the current moment's PPD value $\phi(k)$, a correction step is performed to derive the optimal output estimate $\hat{\phi}_{MI}(k|k)$ of the PMSM at the current moment. Finally, the actual dynamic linearization model of MFAC is updated accordingly.

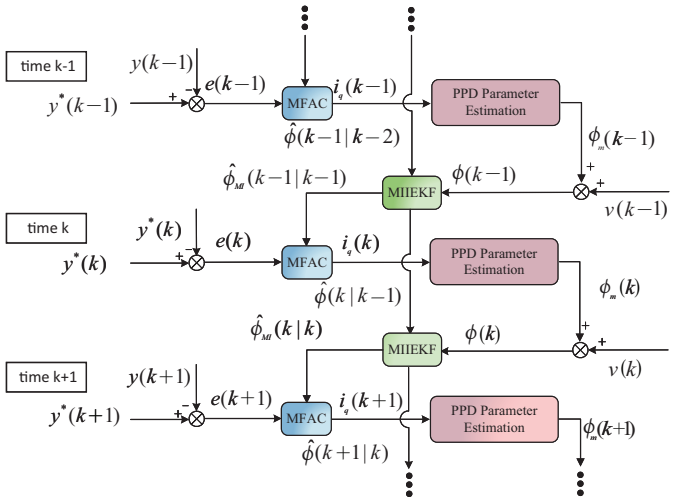

FIGURE 2. Structure of MFAC based on MIIEKF.

4. STABILITY ANALYSIS

Theorem 2 *Under Assumptions 1–3, when the desired speed satisfies* $n^*(k+1) = n^*(k) = \text{const}$, *the PMSM speed tracking error using the MIIEKF-MFAC method converges monotonically, and the system exhibits bounded input and bounded output stability.*

Proof 2 *From (7),* $v(k)$ *denotes the estimation error noise introduced by the modified projection algorithm. According to [13],* $v(k)$ *is bounded, that is,* $v(k) \leq b_1$. *Under Assumption 4, the data model error* $d(k)$ *is bounded. This implies that* $w(k)$ *is also bounded, i.e.,* $w(k) \leq b_2$.

From (18), *the prediction-update error of the pseudo partial derivative is given by:* $e_m(k|k) = \phi_m(k) - \hat{\phi}(k|k)$. *Combining this with Equation (12) leads to:*

$$\begin{aligned} |e_m(k|k)| &= \phi_m(k) - \hat{\phi}(k|k-1) \\ &\quad -K(k)[\phi(k) - \hat{\phi}(k|k-1)]. \end{aligned} \tag{34}$$

From (7), $\phi(k) = \phi_m(k) + v(k)$, *it follows that:*

$$\begin{aligned} |e_m(k|k)| &= \Big|\phi(k) - v(k) - \hat{\phi}(k|k-1) \\ &\quad -K(k)[\phi(k) - \hat{\phi}(k|k-1)]\Big| \\ &= |[1-K(k)]\, e_m(k|k-1) + K(k)v(k)|. \end{aligned} \tag{35}$$

Since (20) indicates $K(k) \in [0,1]$, *we have* $[1-K(k)] \leq 1$. *Given that* $v(k)$ *is bounded by* $v(k) \leq b_1$, *it follows that:*

$$|e_m(k|k)| \leq |e_m(k|k-1)| + |v(k)|. \tag{36}$$

Furthermore, we obtain the following from (23):

$$\begin{aligned} |e_m(k|k)| &\leq \left|1 - \frac{\eta \Delta i_q(k-1)^2}{\mu + \Delta i_q(k-1)^2}\right| |e_m(k-1|k-1)| \\ &\quad + |w(k-1)| + |v(k)|. \end{aligned} \tag{37}$$

Since $\eta \in (0,1]$ *and* $\mu > 0$, *the term* $|1 - \frac{\eta \Delta i_q(k-1)^2}{\mu + \Delta i_q(k-1)^2}|$ *is monotonically decreasing, with a maximum value of* $1 - \frac{\eta \varepsilon^2}{\mu + \varepsilon^2}$.

Thus, there exists a constant m such that:

$$0 \leq \left|1 - \frac{\eta \Delta i_q(k-1)^2}{\mu + \Delta i_q(k-1)^2}\right| \leq 1 - \frac{\eta \varepsilon^2}{\mu + \varepsilon^2} = m < 1. \quad (38)$$

Therefore, (37) *can be rewritten as:*

$$\begin{aligned} |e_m(k|k)| &\leq m\,|e_m(k-1|k-1)| + |w(k-1)| + |v(k)| \\ &\leq m\,|e_m(k-1|k-1)| + b_1 + b_2 \\ &\leq m^2\,|e_m(k-2|k-2)| + (m+1)b_2 + (m+1)b_1 \\ &\leq \cdots \\ &\leq m^{k-1}\,|e_m(1|1)| + (b_1+b_2)\,\frac{(1-m^{k-1})}{1-m} \end{aligned} \quad (39)$$

From Assumption 3, $|\phi(k)| \leq b$, and since $v(k) \leq b_1$, (7) implies that $\phi_m(k)$ is bounded. Given that (39) *shows $|e_m(k|k)|$ is bounded, it follows that $\phi(k|k)$ is bounded.*

As established in Section 2, the standard Kalman filter ensures exponentially stable and bounded estimation error under persistent excitation. The Multi-Innovation Kalman Filter (MIKF) extends this framework by constructing an augmented system through innovation stacking. Since the original system satisfies the boundedness condition for the PPD $\hat{\phi}(k|k)$, this property is preserved in the augmented system. Therefore, according to multi-innovation system theory, the MIIEKF also yields an exponentially stable estimator with uniformly bounded error [14]. Consequently, the PPD estimate $\hat{\phi}_{MI}(k|k)$ obtained from the MIIEKF remains uniformly bounded.

5. EXPERIMENTAL VERIFICATION

To assess the practical effectiveness of the proposed method, a series of experiments was conducted on the experimental platform depicted in Figure 3. This platform includes an upper computer, a motor-drag system, and a multi-motor drive control unit. The test used a PMSM (controlled object) loaded by a DC motor [15]. Its performance was compared with PI [16] and MFAC [17] under two distinct operating conditions. The $i_d^* = 0$ control strategy was performed. The sampling period was set to be 10 µs, and the DC bus voltage was $U_{DC} = 24$ V.

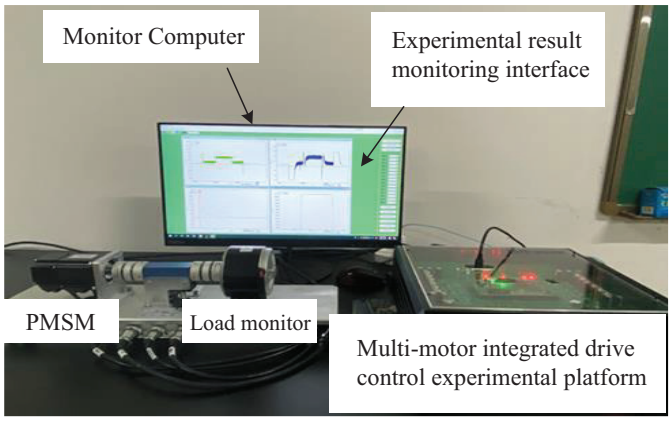

FIGURE 3. Experimental platform.

Table 1 lists the nominal parameters of the PMSM. Table 2 provides the specific control parameters for the PI, MFAC, and MIIEKF-MFAC algorithms.

TABLE 1. Parameters of PMSM.

Parameters	Values
Rated voltage U_N (V)	36
Rated output power P (W)	200
DC voltage U_{DC} (V)	24
Rated Torque T_L (N · m)	0.45
Number of Pole Pair n_p (pairs)	4
Stator resistance R_s (Ω)	0.33
d-axis Stator inductance L_d (mH)	0.9
Rated Speed n_N (r/min)	2500
q-axis Stator inductance L_q (mH)	0.9
Rotor PM flux ψ_r (Wb)	0.0105
Rotational Inertia J (kg · m^2)	1.89×10^{-5}

TABLE 2. Parameters of controllers.

PI	MFAC	MIIEKF-MFAC
$P = 0.03$	$\phi(1) = 2, \lambda = 0.1$	$\hat{\phi}_{MI}(1\|0) = 4, \lambda = 0.2$
$I = 0.77$	$\eta = 0.86, \rho = 0.2$	$\eta = 0.75, \rho = 0.4$
	$\mu = 0.01$	$\beta = 0.5, p = 3$
		$Q = 0.5, R = 3$
		$\mu = 0.01$

$\phi(1)$ and $\hat{\phi}_{MI}(1|0)$ are the initial values of the reset mechanism of the PPD.

5.1. Control Performance of PMSM at Varying Speed and Load

At 3.5 s, the reference speed, n_d, was set to 1000 r/min, and the load torque, T_L, was set to 0.1 N · m. Then, at 4.5 s, the reference speed, n_d, was set to 1500 r/min, and the load torque, T_L was increased to 0.2 N · m. Finally, at 6.0 s, the reference speed, n_d, was set to 2200 r/min, and the load torque, T_L was increased to the rated value of 0.45 N · m.

Figure 4 shows the experimental results comparing conventional PI control, MFAC, and MIIEKF-MFAC methods under variable speed and load conditions. The experimental findings are summarized as follows.

(i) The conventional PI control fails to rapidly track step references during speed regulation. At 4.5 s, the response is characterized by a slow convergence process (0.9 s) accompanied by speed fluctuations of 9 r/min [see Figure 4(a) Magnified area 1]. By 6 s, a maximum speed deviation of 31 r/min is observed [see Figure 4(a) Magnified area 2]. Compared with no-load operation, the control performance deteriorates significantly under varying speed and load conditions.

(ii) At 4.5 s under 1500 r/min, the CFDL-MFAC exhibits faster dynamic response than the PI control, converging

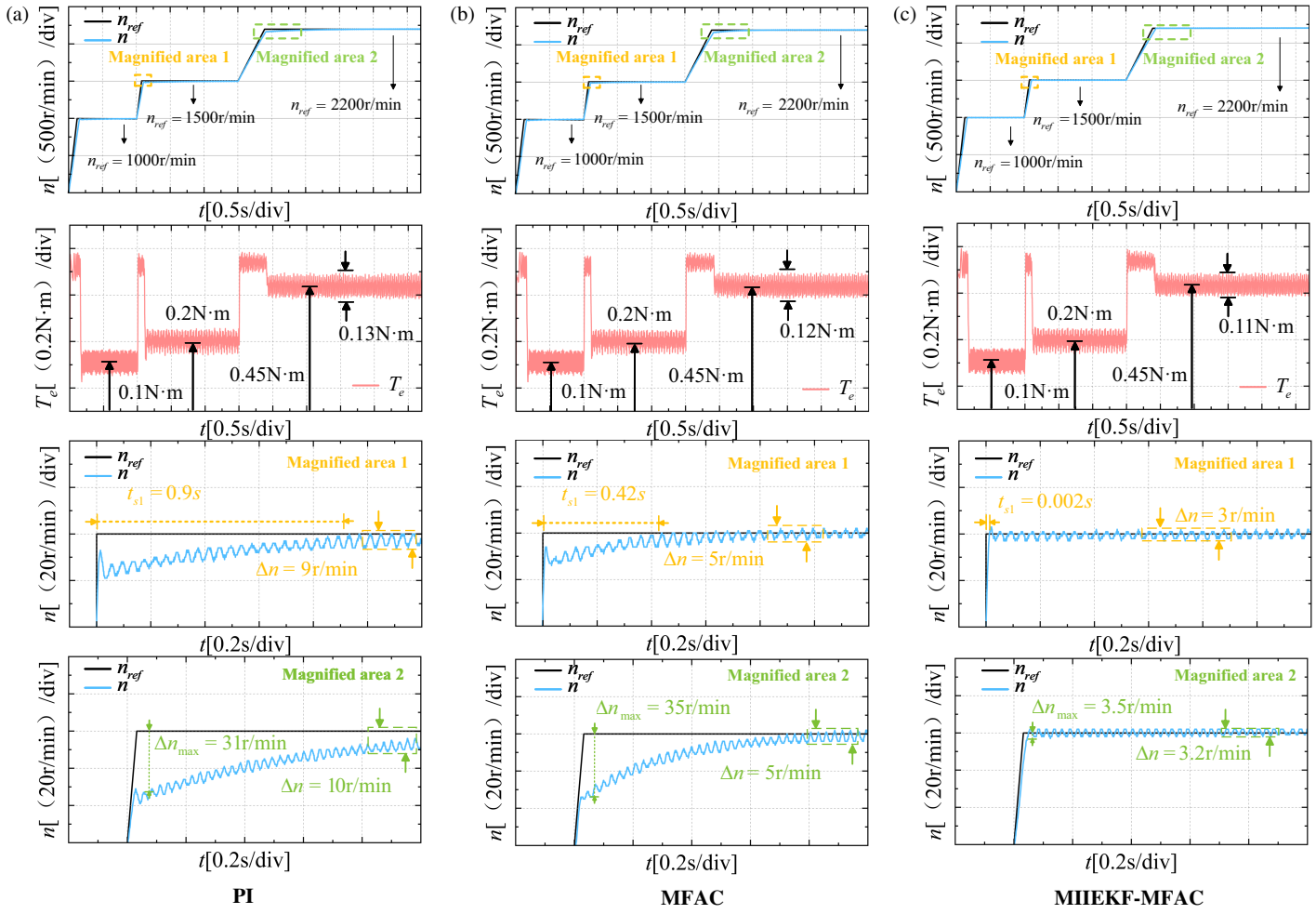

FIGURE 4. Experimental results of the three control algorithms at varying speed and load.

within 0.42 s. Nevertheless, there are still speed oscillations of 9 r/min [see Figure 4(b) Magnified area 1]. At 6 s, the speed deviation reaches a peak value of 35 r/min [see Figure 4(b) Magnified area 2]. The dynamic performance remains unsatisfactory, with noticeable degradation under variable speed and load conditions.

(iii) By comparison, at 4.5 s, MIIEKF-MFAC achieves ultrafast convergence in only 0.002 s, with speed variations limited to 3 r/min [see Figure 4(c) Magnified area 1]. By 6 s, the steady-state error is restricted to 1.6 r/min, and the maximum speed error is merely 3.5 r/min [see Figure 4(c) Magnified area 2]. These results conclusively verify its exceptional robustness under varying speeds and load conditions.

As shown in Figure 4, the MIIEKF-MFAC algorithm demonstrates superior performance in torque ripple suppression, thereby effectively enhancing the operational quality of the system.

5.2. Control Performance of PMSM at Varying Load

The reference speed, n_d, was set to 1,000 r/min and remained constant throughout the operation. During stable motor operation, the load torque, T_L, was increased to the rated value 0.45 N · m at 9 s, and was restored to 0 N · m at 12.5 s.

Figure 5 shows the experimental results of the conventional PI control, MFAC, and MIIEKF-MFAC methods under varying load conditions. The key findings are summarized as follows.

(i) The conventional PI control requires 3 s to achieve stabilization, with a speed fluctuation amplitude of 90 r/min [see Figure 5(a) Magnified areas 1–2].

(ii) The CFDL-MFAC method reduces the settling time to 1.5 s and restricts the maximum speed deviation to 75 r/min [see Figure 5(b) Magnified areas 1–2].

(iii) The MIIEKF-MFAC algorithm achieves stability in only 0.5 s, with a peak speed deviation of merely 39 r/min[see Figure 5(c) Magnified areas 1–2]. These results represent an 83.3% improvement in response speed and a 57% reduction in speed deviation compared to the PI control.

At the 9 s mark, the torque response curves in Figure 5 reveal that both the conventional PI control and CFDL-MFAC exhibit significant current tracking errors and a phase shift of about 1°.

In contrast, the proposed MIIEKF-MFAC strategy demonstrates enhanced dynamic performance, yielding smoother and more stable torque waveforms.

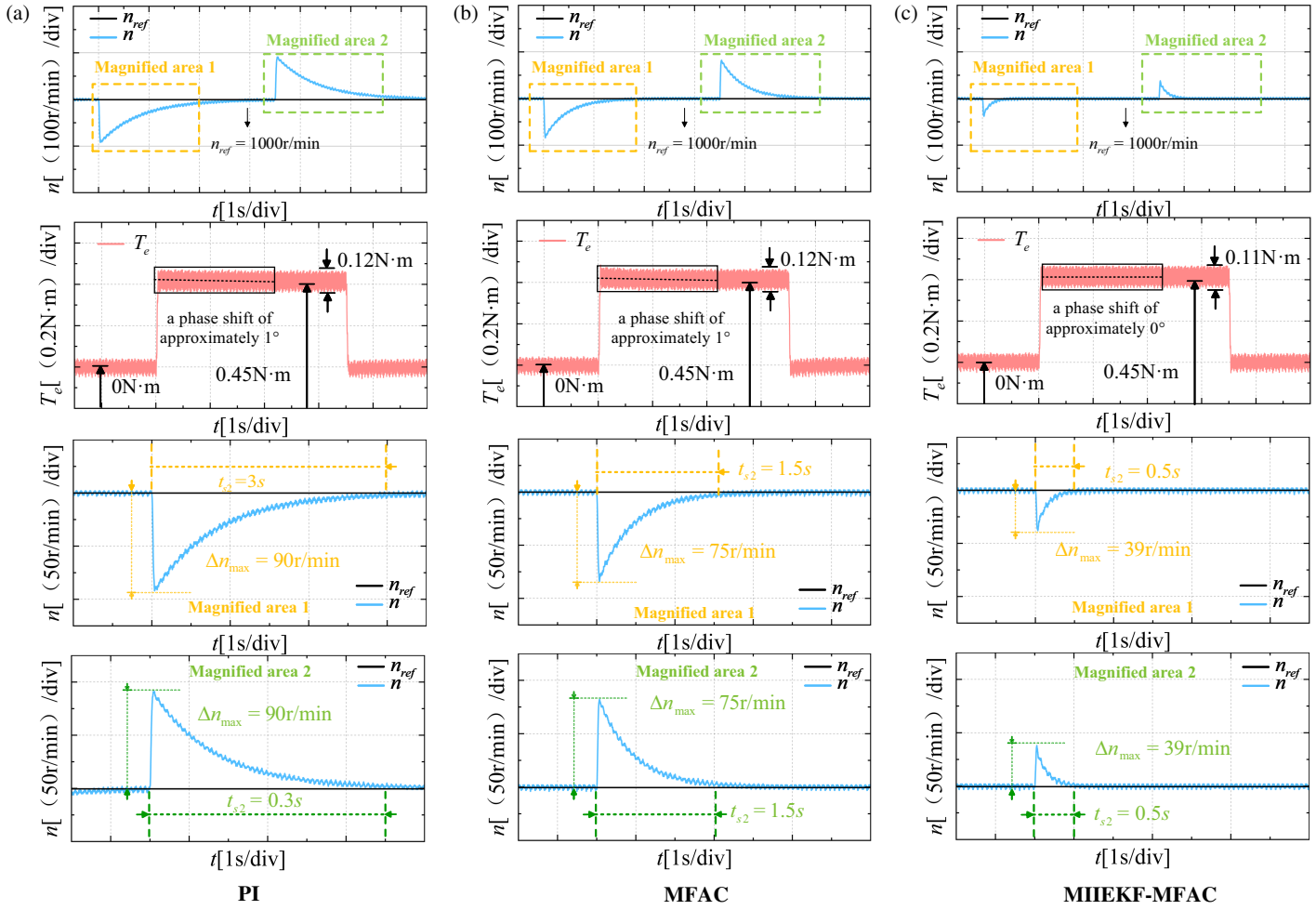

FIGURE 5. Experimental results of the operation of three control algorithms running under sudden load changes.

TABLE 3. Parameters of controllers.

Operating conditions	Operating Parameters	The 1st Stage	The 2st Stage	The 3st Stage
Varying speed and load	Set the Time	3.5 s	4.5 s	6 s
	Speed	1000 r/min	1500 r/min	2200 r/min
	Torque	0.1 N · m	0.2 N · m	0.45 N · m
Sudden loading	Set the Time	0 s	9 s	12.5 s
	Speed	1000 r/min	1000 r/min	1000 r/min
	Torque	0 N · m	0.45 N · m	0 N · m

TABLE 4. Control performance comparison.

Operating conditions	Performance	PI	MFAC	MIIEKF-MFAC
Varying speed and load	Convergence time	0.9 s	0.42 s	0.002 s
	Maximum speed deviation	31 r/min	35 r/min	3.5 r/min
	Speed oscillations	9–10 r/min	5 r/min	3–3.2 r/min
	Torque pulsation	0.13 N · m	0.12 N · m	0.11 N · m
Sudden loading	Convergence time	3 s	1.5 s	0.5 s
	Torque pulsation	0.12 N · m	0.12 N · m	0.11 N · m
	Speed overshoot	90 r/min	75 r/min	39 r/min
	Phase shift	1°	1°	0°

5.3. Experimental Setup and Key Results Presentation

To systematically evaluate the performance of the proposed MIIEKF-MFAC method and ensure the fairness and rigor in comparison with PI and MFAC methods, this section presents and analyzes all experimental settings and key results.

The operating condition settings of the aforementioned experiments were summarized in Table 3. The experimental results of the PI, SMC, and MIIEKF-MFAC were summarized in Table 4.

The comparative evaluation confirms that the MIIEKF-MFAC method outperforms the conventional PI and MFAC approaches in terms of dynamic response speed, steady-state tracking accuracy, and robustness.

6. CONCLUSION

This paper proposes an MIIEKF-based MFAC method. The proposed approach not only eliminates the dependency on precise system models but also resolves the estimation reliability issue of PPD through the improved extended Kalman algorithm, while compensating for inaccuracies in the data model. Furthermore, by integrating multi-innovation identification theory, the Kalman algorithm is optimized to ensure rapid state convergence. Experimental results demonstrate that the proposed method achieves excellent dynamic response performance, effectively suppresses chattering, and enhances system robustness. The method ensures the stable and efficient operation of the PMSM under complex working conditions, thus validating its practical utility. Note that adjusting several key parameters, such as the covariance matrices in the MIIEKF and the weighting factors in the MFAC, requires mutual coordination. Developing intelligent parameter tuning methods to further enhance the adaptability and deployment convenience of the proposed method remains a crucial direction for future research.

ACKNOWLEDGEMENT

This work was supported in part by the National Natural Science Foundation of China under Grants 52572375 and 62303178; in part by the Natural Science Foundation of Hunan Province Grant 2024JJ7139; in part by the graduate research innovation project of Hunan Province Grants CX20251659; and in part by the Teaching Reform Research Project of Hunan Provincial Education Department of China under Grant 202502000971.

REFERENCES

[1] Orlowska-Kowalska, T., M. Wolkiewicz, P. Pietrzak, M. Skowron, P. Ewert, G. Tarchala, M. Krzysztofiak, and C. T. Kowalski, "Fault diagnosis and fault-tolerant control of PMSM drives–state of the art and future challenges," *IEEE Access*, Vol. 10, 59 979–60 024, 2022.

[2] Chen, W., Z. Mao, and W. Tian, "Water cooling structure design and temperature field analysis of permanent magnet synchronous motor for underwater unmanned vehicle," *Applied Thermal Engineering*, Vol. 240, 122243, Mar. 2024.

[3] Singh, A. K., R. Raja, T. Sebastian, and A. Ali, "Limitations of the PI control with respect to parameter variation in PMSM motor drive systems," in *2019 IEEE International Electric Machines & Drives Conference (IEMDC)*, 1688–1693, San Diego, CA, USA, May 2019.

[4] Ke, D., F. Wang, X. Yu, S. A. Davari, and R. Kennel, "Predictive error model-based enhanced observer for PMSM deadbeat control systems," *IEEE Transactions on Industrial Electronics*, Vol. 71, No. 3, 2242–2252, Mar. 2024.

[5] Yin, Z., X. Wang, X. Su, Y. Shen, D. Xiao, and H. Zhao, "A switched ultra-local model-free predictive controller for PMSMs," *IEEE Transactions on Power Electronics*, Vol. 39, No. 9, 10 665–10 669, Sep. 2024.

[6] Davari, S. A., M. S. Mousavi, B. Nikmaram, F. Flores-Bahamonde, F. Wang, P. Wheeler, and J. Rodriguez, "Sensorless model-free predictive control of permanent magnet synchronous motor," *IEEE Transactions on Industrial Electronics*, 1–12, 2025.

[7] Wang, L., S. Zhang, C. Zhang, Y. Huang, Y. Dong, and S. Wang, "An improved model-free adaptive current control for PMSM based on prior-optimization," *IEEE Transactions on Industrial Electronics*, Vol. 72, No. 6, 5591–5601, Jun. 2025.

[8] Chu, W. and X. Shui, "Application of predictive control for synchronous motors in oil field automation," *International Core Journal of Engineering*, Vol. 11, No. 10, 56–65, 2025.

[9] Hou, Z., R. Chi, and H. Gao, "An overview of dynamic-linearization-based data-driven control and applications," *IEEE Transactions on Industrial Electronics*, Vol. 64, No. 5, 4076–4090, 2017.

[10] Cao, Y., X. Ren, Q. Guo, G. Wu, Q. Long, and M. Ran, "Position sensorless control of PMSM based on EKF current noise compensation and MRAS," in *2024 IEEE International Conference on Mechatronics and Automation (ICMA)*, 870–875, Tianjin, China, 2024.

[11] Dan, L., "EKF-based fault detection and isolation for PMSM inverter," *Sustainable Energy Technologies and Assessments*, Vol. 52, 101846, Aug. 2022.

[12] Ding, F., "Least squares parameter estimation and multi-innovation least squares methods for linear fitting problems from noisy data," *Journal of Computational and Applied Mathematics*, Vol. 426, 115107, Jul. 2023.

[13] Hou, Z. and S. Xiong, "On model-free adaptive control and its stability analysis," *IEEE Transactions on Automatic Control*, Vol. 64, No. 11, 4555–4569, Nov. 2019.

[14] Xiao, J., Y. Xiong, Y. Zhu, C. Zhang, T. Yi, X. Qian, Y. Fan, and Q. Hou, "Multi-innovation adaptive Kalman filter algorithm for estimating the SOC of lithium-ion batteries based on singular value decomposition and Schmidt orthogonal transformation," *Energy*, Vol. 312, 133597, Dec. 2024.

[15] Lim, S., "Sensorless-FOC for PMSM with single DC-link shunt," Application Note, Texas Instruments, 1–32, 2020.

[16] Vas, P., *Sensorless Vector and Direct Torque Control*, Oxford University Press, 1998.

[17] Hou, Z. and S. Jin, *Model Free Adaptive Control*, CRC Press, Boca Raton, FL, USA, 2013.